

Response to Reviewer Comments for “Urban aerosol chemistry at a land-water transition site during summer – Part 2: Aerosol pH and liquid water content” by Michael A. Battaglia Jr. et al., Atmos. Chem. Phys. Discuss., <https://doi.org/10.5194/acp-2021-368-RC1>, 2021”

We thank the reviewers for their detailed and helpful comments. We have addressed each comment with the Referee comments in bold and our reply in plain text immediately below. We provide at the end the edited manuscript with all changes highlighted.

REVIEWER #1

Major Comments

1.) It looks necessary to quantify the impact of measurement uncertainties to these two pH calculation methods. The authors should also provide the QA/QC information, not only limited to concentrations, but also the impact on possible ranges of pH calculated.

We have attempted to address this issue by referring readers to the literature. Additional discussion of the impact on calculated aerosol pH based on uncertainty in the measured input concentrations have been added. The following discussion was added at the conclusion of the Methods section of the paper to elaborate on these uncertainties:

“Commonly, a reasonable estimate of measurement errors associated with the species of interest are on the order of 15% + 1 nmol m⁻³ for online sampling methods (Murphy et al. 2017). Utilizing this estimate in the extreme acidic case (ambient observed SO₄²⁻ and NO₃⁻ adjusted to + 15% + 1 nmol m⁻³; NH₄⁺ adjusted to – 15% – 1 nmol m⁻³) or non-acidic case (SO₄²⁻ and NO₃⁻ adjusted down by – 15% – 1 nmol m⁻³ and NH₄⁺ adjusted up by + 15% + 1 nmol m⁻³), the uncertainty of aerosol pH was predicted to vary by 0.1 – 1 pH units (Murphy et al. 2017). Similarly, Pye et al. (2020) reported that in cases for RH above 60% deviations of the ISORROPIA-predicted pH and the IUPAC-defined pH are less than one pH unit. The present calculations have similar uncertainties in the pH calculations.”

2.) Line 107-108: Is it because how pH was defined (e.g. pH_c or pH_m in Jia et al. (2018))? It’s better to clarify how the pH was defined in the first place.

This statement has been clarified to reflect that the methods of Hennigan et al. 2015 and Zheng et al. 2020 are identical with the exception of the values of the equilibrium constants used. Based on our investigation, the non-ideality corrections introduced in Zheng et al. 2021 appear to be working towards ISORROPIA, but instead of calculating activity coefficients they interpolate with thermodynamic outputs from ISORROPIA (or E-AIM if desired) to try to mimic the thermodynamic models based on what they say impacts non-ideality the most (they base it on T, RH, and NO_3^-). The text has been updated to read:

“The method of Zheng et al. (2020) is based upon a similar approach in prior studies (Hennigan et al., 2015; Keene et al., 2004); the two methods are identical, with the minor differences a result of equilibrium constant values used based on ranges provided in the literature.”

3.) *Line 153: Looks like the authors intend to make comparisons of pH in different locations and discuss the influence from RH and T, but I did not see such discussions in the following discussion. I think the authors should clarify what “strong implications” they are referring to.*

The differences between locations were intended to describe the changes in diurnal T, RH, and ALWC between the Baltimore (urban) and HMI sites. The unique character of these profiles at the HMI site (neither strongly urban nor rural) was investigated as a driver of the model-predicted aerosol pH during the OWLETS 2 study. The discussion points have been linked together, and the original statement on Line 153 has been changed to read:

“The differences shown in Fig. 1 were due to the proximity of HMI to the Chesapeake Bay and have several implications for aerosol pH, which will be discussed in detail below.”

4.) *Line 162-171: NH₃ phase partitioning also strongly depends on the availability of accompanied acids. Without balance ions, NH₃ alone cannot form particles. On the other hand, for pure ammonium sulfate, the evaporation tendency of NH₃ is also quite limited. Low concentrations of particulate acids could also lead to ammonia-rich atmosphere.*

We have attempted to address this comment together with Reviewer 2 Major Comment #2. Please see the response to Reviewer 2 Major Comment #2 for details.

5.) *Figure 4 &5: These two figures provide valuable local information about pH response and of high importance for similar studies comparison. As a result, the authors should provide a more complete description about how the data points are chosen, averaged or processed. The authors have 20-minutes resolution data, while only 8 points are plotted. How were the bins chosen and why not just use all the measured data?*

Figures 4 and 5 have been expanded to display both the binned data (from the original manuscript) together with the entire collection of raw unbinned data used to generation the original figures to show any relevant trends. We have clarified the binning process by describing the maximum number of points permitted in each bin by addition of the following text to the figure captions:

“Figure 4: Relationship between aerosol pH and (a) temperature, (b) aerosol liquid water, and (c) total NH_3 ($\text{Tot-NH}_3 = \text{NH}_3 + \text{NH}_4^+$). Symbols represent mean values while error bars represent standard deviations; bins were limited to a maximum of 160 points per bin.”

“Figure 5: Relationship between NH_3 partitioning ($\epsilon_{\text{NH}_3} = \text{NH}_3/(\text{NH}_3 + \text{NH}_4^+)$) and aerosol liquid water. Symbols represent mean values while error bars represent standard deviations,; bins were limited to a maximum of 160 points per bin.”

6.) *Line 225-231: Either high RH or high particle mass loading can be responsible for high ALWC, while it’s hard to say the later case corresponds to the dilution effect. Could the authors distinguish which one dominates the ALWC? In the latter discussion, the authors mentioned the particles were likely externally mixed, so that the ALWC involved in the NH_3 phase partitioning processes should be, more or less, overestimated. Should that be considered here as well?*

Reviewer 2 expressed a related sentiment in Minor Comment #5 (Lines 228-240 of the original manuscript). While the additional discussion of that comment addresses, more specifically the surprising result of seemingly contradictory findings on relatively invariant pH with both

increasing NH_3 and ALWC, we have also added clarifying statements to address this comment as well. The following comment has been added at the end of line 227 of the original manuscript:

“A combination of particle mass loading, aerosol composition, and ambient RH are responsible for the variations in ALWC.”

Additionally, it should be noted that previous studies have shown that the ALWC predictions of aerosol thermodynamic equilibrium models are highly accurate. For example, Guo et al. (2015) observed excellent agreement between model-predicted ALWC and direct observations during the SOAS campaign. This is one of the key parameters evaluated when a new model is published (e.g., Fountoukis and Nenes, 2007). This is further supported by the results of Ansari and Pandis (1999), who found generally excellent agreement in ALWC predictions between four different thermodynamic equilibrium models, even when predictions of other semivolatile species did not agree.

Minor Comments

1.) Introduction: it's better to mention some current existing methods of pH direct Measurement.

We have added the following discussion regarding the existing method of aerosol pH direct measurement:

“However, direct measurements of aerosol pH remain challenging. Single particle studies of aerosol pH using Raman spectroscopy have been performed, but are limited by the presence of both HSO_4^- and SO_4^- limiting their application to more acidic particles (Boyer et al., 2020; Rindelaub et al., 2016). Colorimetric measurements of aerosol pH have also been employed, but such techniques have been limited to laboratory studies with relatively simple aerosol compositions (Craig et al., 2018; Jang et al., 2020).”

2.) Line 49: I do not follow the logic here, how does the previous sentence explain the later?

The sentences were intended to be linked based on the controlling regimes of NH₃ influence on aerosol pH, *i.e.*, the compositionally-controlled or meteorologically-controlled. The statements have been linked and clarified in the following manner and the text now reads:

“NH₃ partitioning is controlled by the concentration of strong acids and by the ambient temperature and relative humidity, hence, the dependence of pH on both composition and meteorology (Zheng et al., 2020). In some regimes, the meteorological factors are more important than the compositional factors, explaining why NH₃ can exist partially in the gas phase even when the aerosol pH is highly acidic (Nenes et al., 2020; Weber et al., 2016).”

3.) Figure 7: Should the relative concentrations of nitrate be more reflective to the Cl displacement extent than absolute concentrations? And on this Figure, about half the data points have Cl:Na >1, what's the possible explanation?

We do not feel that the relative concentrations of nitrate are more reflective to the Cl displacement extent than absolute concentrations. The additional components of sampled PM mass may have effects on the relative concentrations, but are unlikely to play a part in the actual displacement reaction. Regarding the Cl:Na > 1 condition present, our expectation is that there is an additional source of Cl that is difficult to account for, such as combustion sources from the similar industrial point sources documented in the Part 1 manuscript, local boat traffic, or equipment and truck traffic associated with work activities on Hart-Miller Island. Because we do not have a way to identify the additional Cl source, such discussion would be speculative.

REVIEWER #2 RESPONSES

Major Comments

1.) Given the poor performance of ISORROPIA for NH₃ partitioning predictions (pH dependent) in this study, Eq. 1-Eq. 3 was used to calculate aerosol pH, and the pH calculated from these equations was significantly different from the ISORROPIA-predicted aerosol pH. However, these equations are for ideal conditions (without considering ion activity coefficients), and the non-ideality in aerosols can introduce deviations from the ideal conditions. Zheng et al. (<https://doi.org/10.5194/acp-2021-55>) has recently introduced a non-ideality correction factor for using these equations to calculate aerosol pH, and the aerosol pH calculated from the non-ideality corrected equations agreed well with the pH value determined by ISORROPIA.

Therefore, I suggest the authors to use the non-ideality corrected equations (either with non-ideality correction factor or with the related ion activity coefficients) to calculate aerosol pH and then compare with ISORROPIA predicted pH.

In Zheng et al. (2021), the goal is to account for non-idealities in the thermodynamic calculation of pH based on ammonia partitioning. Note that Zheng et al. (2020) performed their calculations assuming ideal conditions. The non-ideality treatment of Zheng et al. (2021) is not actually thermodynamic model output, but is estimated based on three factors that are determined to impact non-ideality: temperature, RH, and the fraction of particulate anions contributed by nitrate. The estimation occurs then by interpolating from tables generated from thermodynamic models like ISORROPIA and E-AIM.

This correction was carried out on our data here. The ISORROPIA-generated thermodynamic lookup tables were used and the pH_f (partitioning, non-ideal) were calculated and compared to the pH_f (partitioning, ideal). While the non-ideality correction increases the correlation with ISORROPIA-calculated pH, we chose to not include it for three reasons: (1) the correction is based on interpolation from ISORROPIA outputs and attempts to mimic its output with more computational efficiency than running the full model; however, we do not need to mimic

ISORROPIA, as we have all of the necessary inputs and have already run it in full. We use the ammonia partitioning method as a completely independent thermodynamic calculation. That being said, we acknowledge that the method used here is based on an ideal assumption (the same assumption of ideality used throughout Zheng et al., Science, 2020). (2) The absolute impact on the pH calculated is not severe and does not impact the conclusions of the work (on average, a difference of ~0.5 pH units between partitioning ideal and partitioning non-ideal was observed). (3) Finally, we appreciate the Referee's comment and alerting us to this very recent manuscript. Given that Zheng et al. (2021) is currently under review, we feel that it would be premature to adopt their methodology before it has passed the peer-review process. If substantial changes in their manuscript occur during revision (or if the manuscript is not accepted for publication), this would have serious implications for our conclusions if we adopt their methodology.

2.) Fig. 4, shows the relationship between aerosol pH and factors such as temperature, aerosol liquid water and total NH₃. It seems that the influence of one factor on pH can also be affected by other factors. Is it possible to vary one factor with fixed other factors to investigate the influence of one factor?

Pye *et al.* (2020) address this question in Table S3 of the accompanying supplemental information. For five aerosol thermodynamic equilibrium models (E-AIM model III, AIOMFAC-GLE, MOSAIC, ISORROPIA II, and EQUISOLV II), the authors make predictions of molality-based pH and related properties for the water + (NH₄)₂SO₄ + H₂SO₄ + NH₃ system at 298.15 K. For the case of their 'moderately acidic' water-free input system, increasing RH from 40% to 99% was demonstrated to increase ISORROPIA II-predicted aerosol pH from 1.84 to 4.47, with a corresponding change in the hydronium ion activity coefficient. For the 'highly acidic' water-free composition input (50% (NH₄)₂SO₄ by mass, with less NH₃), similar change in RH resulted in aerosol pH increasing from -0.15 to 2.54.

While this experiment was performed with idealized systems, as described in the main body of their manuscript, we would expect similar findings with our observational results, *e.g.* increasing RH would increase aerosol pH at fixed concentration, and increasing the acidic components of

the aerosol would decrease aerosol pH for fixed RH. However, doing so for our observations may not have much meaning, as ambient T, RH, and aerosol composition are fixed inputs at each time point for model inputs to predict aerosol pH.

Additionally, Tao and Murphy (2021), and Zhou et al. (2021), demonstrated the effects of individual drivers of aerosol pH on both diurnal and monthly/seasonal time frames utilizing ambient data by systematically decomposing the pH calculation. In most cases, temperature was the single largest driver, followed by NH₃ concentration, ambient RH, and aggregate particle properties in decreasing order of effect. Tao and Murphy (2021) found that temperature was the single largest driver of pH, followed by (in decreasing order of effect) the NH₃ effect (opposite the T effect), RH, and particle properties in Toronto, Canada. Likewise Zhou et al. (2021) found that temperature was the primary driver, both across seasons and day/night cycles, followed (generally) by the NH_x effect, then RH and occasionally SO₄²⁻, and during certain periods of the diurnal cycle, the NVC effect in decreasing order of effect.

Minor Comments

1.) In Fig. S4, it would be better to use the same y scale when comparing pH values determined from different methods.

We have combined the axes of the plots, ensuring the scales on the figure are identical for better comparison of the pH values.

2.) Line 228-240: “The result shown in Fig. 4b is somewhat surprising because NH₃ partitioning was quite sensitive to ALWC (Fig. 5); the relatively invariant aerosol pH is unexpected given the increase in NH₃ uptake in the presence of ALW.” A discussion of this surprising result would be useful. (The following discussion in the manuscript about the dry deposition is not very relevant to this result).

We have retained the discussion on dry deposition, as we feel it is valuable to the overall discussion of aerosol pH (though not necessarily to the point we intend to make), but we have added additional discussion related to the surprising result as requested by the reviewer. The following discussion has been added to elaborate on the point we intended to make:

“With increasing NH_3 uptake in the presence of, and simultaneous with, the increased ALWC, it would be anticipated that aerosol pH would become more basic both through the reaction of NH_3 to form NH_4^+ and due to the dilution effect of liquid water. However, the results of Figures 4 and 5 reveal that despite both the increase in NH_3 uptake and increase ALWC, aerosol pH remains relatively unchanged, with only a 0.5 pH unit change at the highest values of ALWC.”

This change also contains additional clarification to address Reviewer 1 Major Comment #6 as described above.

3.) *Line 296-298: ISORROPIA didn't give good NH_3 partitioning predictions in this study and the different chemical compositions of the coarse- and fine-mode particles were used to explain it. I think the explanation is reasonable, however, I was still wondering what result you will get with E-AIM calculations. If the E-AIM also fails to predict NH_3 partitioning here, this explanation would be more solid since E-AIM also assumes an internally mixed aerosol distribution.*

Making comparisons of ISORROPIA and E-AIM calculations is outside the scope of this particular work, and would be repeating work performed in recent studies. Notably, Pye et al. (2020) comprehensively compared multiple aerosol thermodynamic equilibrium models for consistency. In polluted environments, such as Mexico City, aerosol pH predictions obtained from E-AIM, ISORROPIA, and the NH_3 partitioning approach were shown to be in good agreement. Under both the moderately and highly acidic conditions described in Pye et al. (2020), E-AIM and ISORROPIA predicted values never exceeded 1 pH unit difference, and then only at low (<50% RH) values; for values above 60% RH this difference was on the order of 0-0.5 pH units. Exact values are given in Table 6 of Pye et al. (2020).

The pH of coarse-mode particles is anticipated to be higher than for fine-mode particles owing to the enrichment of the coarse-mode with NVCs from dust and sea salt. Differences of up to 4 pH units have been shown between fine- and coarse-modes. As E-AIM and ISORROPIA are shown to be in acceptable agreement at the observed ambient RH ranges in the present study (RH > 60%), it should be expected that ISORROPIA would more accurately predict the aerosol pH

when the coarse mode is included from an internally-mixed standpoint as E-AIM lacks NVC constituents as inputs.

References

- Ansari, S. & Spyros N. Pandis (1999). An Analysis of Four Models Predicting the Partitioning of Semivolatile Inorganic Aerosol Components, *Aerosol Science and Technology*, 31:2-3, 129-153.
- Boyer, H. C., Gorkowski, K., & Sullivan, R. C. (2020). In Situ pH Measurements of Individual Levitated Microdroplets Using Aerosol Optical Tweezers. *Analytical Chemistry*, 92(1), 1089-1096. <https://doi.org/10.1021/acs.analchem.9b04152>
- Craig, R. L., Peterson, P. K., Nandy, L., Lei, Z., Hossain, M. A., Camarena, S., Dodson, R. A., Cook, R. D., Dutcher, C. S., & Ault, A. P. (2018). Direct Determination of Aerosol pH: Size-Resolved Measurements of Submicrometer and Supermicrometer Aqueous Particles. *Analytical Chemistry*, 90(19), 11232-11239. <https://doi.org/10.1021/acs.analchem.8b00586>
- Fountoukis, C. and Nenes, A.: ISORROPIA II: a computationally efficient thermodynamic equilibrium model for K^+ - Ca^{2+} - Mg^{2+} - NH_4^+ - Na^+ - SO_4^{2-} - NO_3^- - Cl^- - H_2O aerosols, *Atmos. Chem. Phys.*, 7, 4639–4659, <https://doi.org/10.5194/acp-7-4639-2007>, 2007.
- Hennigan, C. J., Izumi, J., Sullivan, A. P., Weber, R. J., & Nenes, A. (2015). A critical evaluation of proxy methods used to estimate the acidity of atmospheric particles. *Atmos. Chem. Phys.*, 15(5), 2775-2790. <https://doi.org/10.5194/acp-15-2775-2015>
- Jang, M., Sun, S., Winslow, R., Han, S., & Yu, Z. (2020). In situ aerosol acidity measurements using a UV–Visible micro-spectrometer and its application to the ambient air. *Aerosol Science and Technology*, 54(4), 446-461. <https://doi.org/10.1080/02786826.2020.1711510>
- Keene, W. C., Pszenny, A. A. P., Maben, J. R., Stevenson, E., & Wall, A. (2004). Closure evaluation of size-resolved aerosol pH in the New England coastal atmosphere during summer. *J. Geophys. Res.-Atmos.*, 109(D23), D23307, Article D23307. <https://doi.org/10.1029/2004jd004801>
- Nenes, A., Pandis, S. N., Weber, R. J., & Russell, A. (2020). Aerosol pH and liquid water content determine when particulate matter is sensitive to ammonia and nitrate availability. *Atmos. Chem. Phys.*, 20(5), 3249-3258. <https://doi.org/10.5194/acp-20-3249-2020>
- Rindelaub, J. D., Craig, R. L., Nandy, L., Bondy, A. L., Dutcher, C. S., Shepson, P. B., & Ault, A. P. (2016). Direct Measurement of pH in Individual Particles via Raman Microspectroscopy and Variation in Acidity with Relative Humidity. *J. Phys. Chem. A*, 120(6), 911-917. <https://doi.org/10.1021/acs.jpca.5b12699>
- Weber, R. J., Guo, H., Russell, A. G., & Nenes, A. (2016). High aerosol acidity despite declining atmospheric sulfate concentrations over the past 15 years [Letter]. *Nature Geoscience*, 9(4), 282-285. <https://doi.org/10.1038/ngeo2665>
- Zheng, G., Su, H., Wang, S., Andreae, M. O., Pöschl, U., & Cheng, Y. (2020). Multiphase buffer theory explains contrasts in atmospheric aerosol acidity. *Science*, 369(6509), 1374. <https://doi.org/10.1126/science.aba3719>
- Zheng, G., Su, H., Wang, S., Pozzer, A., and Cheng, Y.: Impact of non-ideality on reconstructing spatial and temporal variations of aerosol acidity with multiphase buffer theory, *Atmos. Chem. Phys. Discuss.* [preprint], <https://doi.org/10.5194/acp-2021-55>, in review, 2021.

Urban aerosol chemistry at a land-water transition site during summer – Part 2: Aerosol pH and liquid water content

M. A. Battaglia, Jr.^{1,a}, N. Balasus¹, K. Ball¹, V. Caicedo², R. Delgado², A. G. Carlton³, and C. J. Hennigan^{1*}

¹Department of Chemical, Biochemical, and Environmental Engineering, University of Maryland, Baltimore County

²Joint Center for Earth Systems Technology, University of Maryland, Baltimore County

³Department of Chemistry, University of California, Irvine

^aCurrent affiliation: School of Earth and Atmospheric Sciences, Georgia Institute of Technology

Correspondence: C. J. Hennigan (hennigan@umbc.edu)

1 Abstract

2
3 Particle acidity (aerosol pH) is an important driver of atmospheric chemical processes
4 and the resulting effects on human and environmental health. Understanding the factors that
5 control aerosol pH is critical when enacting control strategies targeting specific outcomes. This
6 study characterizes aerosol pH at a land-water transition site near Baltimore, MD during summer
7 2018 as part of the second Ozone Water-Land Environmental Transition Study (OWLETS-2)
8 field campaign. Inorganic fine mode aerosol composition, gas-phase NH₃ measurements, and all
9 relevant meteorological parameters were used to characterize the effects of temperature, aerosol
10 liquid water (ALW), and composition on predictions of aerosol pH. Temperature, the factor
11 linked to the control of NH₃ partitioning, was found to have the most significant effect on aerosol
12 pH during OWLETS-2. Overall, pH varied with temperature at a rate of -0.047 K⁻¹ across all
13 observations, though the sensitivity was -0.085 K⁻¹ for temperatures > 293 K. ALW had a minor

14 effect on pH, except at the lowest ALW levels ($< 1 \mu\text{g m}^{-3}$) which caused a significant increase
15 in aerosol acidity (decrease in pH). Aerosol pH was generally insensitive to composition (SO_4^{2-} ,
16 $\text{SO}_4^{2-}:\text{NH}_4^+$, $\text{Tot-NH}_3 = \text{NH}_3 + \text{NH}_4^+$), consistent with recent studies in other locations. In a
17 companion paper, the sources of episodic NH_3 events (95th percentile concentrations, $\text{NH}_3 > 7.96$
18 $\mu\text{g m}^{-3}$) during the study are analyzed; aerosol pH was higher by only ~ 0.1 - 0.2 pH units during
19 these events compared to the study mean. A case study was analyzed to characterize the
20 response of aerosol pH to nonvolatile cations (NVCs) during a period strongly influenced by
21 primary Chesapeake Bay emissions. Depending on the method used, aerosol pH was estimated
22 to be either weakly (~ 0.1 pH unit change based on NH_3 partitioning calculation) or strongly
23 (~ 1.4 pH unit change based on ISORROPIA thermodynamic model predictions) affected by
24 NVCs. The case study suggests a strong pH gradient with size during the event and underscores
25 the need to evaluate assumptions of aerosol mixing state applied to pH calculations. Unique
26 features of this study, including the urban land-water transition site and the strong influence of
27 NH_3 emissions from both agricultural and industrial sources, add to the understanding of aerosol
28 pH and its controlling factors in diverse environments.

29 **1 Introduction**

30
31 The acidity, or pH, of atmospheric aerosols affects the chemical and physical properties
32 of airborne particles, and thus, their impacts on climate and health (Pye et al., 2020). The gas-
33 particle partitioning of semi-volatile acidic and basic compounds – notably NH_3 , HNO_3 , HCl ,
34 and organic acids – depends in part on aerosol pH, which directly affects the particulate matter
35 (PM) mass concentration (Nenes et al., 2020). The solubility of many particulate components is
36 pH-dependent, including metals and nutrients, with implications for particle toxicity and nutrient
37 deposition to ecosystems (Fang et al., 2017; Kanakidou et al., 2016). The optical properties of
38 light-absorbing organic compounds, known as brown carbon, can exhibit a strong pH-
39 dependence, which directly affects their climate impacts (Phillips et al., 2017). However, direct
40 measurements of aerosol pH remain challenging. Single particle studies of aerosol pH using
41 Raman spectroscopy have been performed, but are limited by the presence of both HSO_4^- and
42 SO_4^- limiting their application to more acidic particles (Boyer et al., 2020; Rindelaub et al.,
43 2016). Colorimetric measurements of aerosol pH have also been employed, but such techniques
44 have been limited to laboratory studies with relatively simple aerosol compositions (Craig et al.,
45 2018); (Jang et al., 2020). Given the importance of aerosol pH for atmospheric processes and the
46 limitation in estimating acidity with proxies (e.g., ion balances), there has been increased effort
47 in recent years to identify the factors that affect pH and to characterize temporal and spatial
48 variations in the atmosphere (Hennigan et al., 2015).

49 Globally, aerosol pH is often quite acidic due to the ubiquity and abundance of strong
50 acids like H_2SO_4 , HNO_3 , and HCl (Pye et al., 2020). Ammonia (NH_3) is unique among species
51 that affect pH because it is the most abundant basic compound in the atmosphere. NH_3
52 partitioning is controlled by the concentration of strong acids and by the ambient temperature

53 and relative humidity, hence, the dependence of pH on both composition and meteorology
54 (Zheng et al., 2020). In some regimes, the meteorological factors are more important than the
55 compositional factors, explaining why NH₃ can exist partially in the gas phase even when the
56 aerosol pH is highly acidic (Nenes et al., 2020; Weber et al., 2016). Due to its abundance and
57 semi-volatile properties, NH₃ was identified as the most important buffering agent in aerosols
58 across locations with diverse emissions, composition, and climatology (Zheng et al., 2020). In
59 single-phase aqueous particles, organic compounds have a minor effect on pH (Battaglia Jr et al.,
60 2019), though this is not the case for particles that have undergone liquid-liquid phase separation
61 (Pye et al., 2018). Non-volatile cations (NVC) typically contribute a minor fraction of PM mass
62 but can be critical for accurate predictions of pH, especially if NVC concentrations are
63 overestimated (Vasilakos et al., 2018). Globally, NVC are most important in regions heavily
64 impacted by dust emissions (Pye et al., 2020), but have minor effects on pH in other regions (Tao
65 & Murphy, 2019; Zheng et al., 2020).

66 Aerosol pH is also strongly affected by meteorological factors. Equilibrium constants,
67 including those that determine the gas-particle partitioning and aqueous dissociation of semi-
68 volatile acids and bases, are temperature dependent. Temperature is a dominant factor driving
69 variability in the seasonal and diurnal cycling of pH (Guo et al., 2015; Tao & Murphy, 2019).
70 Temperature gradients, as occur in and around urban areas, can also drive large differences in
71 pH, even if the composition is uniform over the same scales (Battaglia et al., 2017). Relative
72 humidity (RH) regulates aerosol liquid water content (ALWC), which affects the partitioning of
73 soluble gases and aqueous phase solute concentrations. ALWC may be the most important
74 factor responsible for large pH differences observed between the southeast US (pH ~0.5-1.0) and
75 the heavily polluted North China Plain (pH ~4-5), the two regions where pH has been most

76 extensively studied to-date (Zheng et al., 2020). These effects can be complex, or even partially
77 offset. For example, an increase in temperature reduces pH owing to the shift in NH_3
78 partitioning towards the gas phase, but NH_3 emissions increase with temperature as well,
79 producing an increase in pH and partially offsetting the pH changes due to temperature (Tao,
80 2020). More research is needed to better understand how all these factors together affect pH, and
81 how this changes geographically and temporally.

82 In this study aerosol pH was characterized during the summertime (4 June to 5 July,
83 2018) at a land-water transition site near a large urban area (Baltimore, MD) as part of the
84 OWLETS-2 (second Ozone Water-Land Environmental Transition Study) field campaign. This
85 site is unique because meteorological phenomena, such as the bay breeze, affect pollution
86 dispersion and recirculation (Loughner et al., 2014). Baltimore is impacted by different regional
87 emission sources, as it is located in the populous and heavily trafficked I-95 corridor, downwind
88 of the Ohio River Valley (He et al., 2013), and relatively close to regional agricultural operations
89 that emit large amounts of NH_3 (Pinder et al., 2006). In a companion paper, the local sources of
90 NH_3 during the OWLETS-2 study were examined, including an analysis of transient events with
91 unexpectedly high NH_3 concentrations (Balasus et al., 2021). In this study, the effects of the
92 observed NH_3 concentrations (including the aforementioned transient concentrations of
93 unexpectedly high values), in combination with the unique meteorological phenomena associated
94 with the land-water transition, on ALW and aerosol pH were investigated.

95

96 **2 Methods**

97 The OWLETS-2 study was conducted to characterize effects of meteorological
98 phenomena associated with the land-water transition on summertime air quality in Baltimore.

99 Hart-Miller Island (HMI, coordinates 39.2421°, -76.3627°), a site located on the Chesapeake Bay
100 ~10 km east of downtown Baltimore, hosted many of the ground-based measurements during the
101 study (Fig. S1). Semi-continuous measurements of aerosol inorganic chemical composition and
102 gas-phase NH₃ were conducted at HMI. The measurement details are provided in the companion
103 paper (Balasus et al., 2021). Briefly, the water-soluble ionic components of PM_{2.5} were
104 measured with a Particle-into-Liquid Sampler coupled to a dual Ion Chromatograph (PILS-IC,
105 Metrohm) operated according to Valerino et al. (2017). NH₃ was measured with an AiRRmonia
106 Analyzer (RR Mechatronics) (Norman et al., 2009). Meteorological parameters were measured
107 with a Vaisala MAWS201 Met Station at 1-minute resolution.

108 The 5-minute NH₃ measurements and 1-minute meteorological measurements were
109 averaged to the 20-minute sampling time of the PILS-IC. Aerosol pH for each 20-min sample
110 was calculated according to the NH₃ partitioning method presented in Zheng et al. (2020). This
111 method uses the relevant temperature-dependent equilibrium constants and the measured
112 concentrations of NH₃ and NH₄⁺ to calculate pH. The method of Zheng et al. (2020) is based
113 upon a similar approach in prior studies (Hennigan et al., 2015; Keene et al., 2004); the two
114 methods are identical, with minor differences only due to equilibrium constant values used based
115 on ranges provided in the literature. Indeed, very close agreement was observed (slope = 0.967,
116 R² = 0.977, n = 872) in calculated pH between the NH₃ partitioning methods of Zheng et al.
117 (2020) and Hennigan et al. (2015). The aqueous phase NH₄⁺ concentration is derived from the
118 mass concentration of NH₄⁺ from the PILS-IC and the ALWC. The ISORROPIA-II
119 thermodynamic equilibrium model was used to calculate ALWC using the PILS-IC, NH₃, and
120 meteorological data as inputs (Fountoukis & Nenes, 2007). The model was run in forward mode

121 (NH₃ and aerosol NH₄⁺ were input at total NH₃) using the metastable assumption according to
122 the recommendation of Guo et al. (2015).

123 Although ISORROPIA can provide pH, the NH₃ partitioning method was used for pH
124 calculations in this study:

$$125 \quad pH = pK_{a,NH_3}^* + \log_{10} \frac{[NH_3(aq)] + [NH_3(g)]}{[NH_4^+(aq)]} \quad (1)$$

$$126 \quad [NH_3(g)] = \frac{p_{NH_3} \rho_w}{RT AWC} \quad (2)$$

$$127 \quad K_{a,NH_3}^* = \frac{[H^+(aq)]([NH_3(aq)] + [NH_3(g)])}{[NH_4^+(aq)]} = K_{a,NH_3} \left(1 + \frac{\rho_w}{H_{NH_3} RT AWC} \right) \quad (3)$$

128 where in Equation 1, [NH₃(aq)] is the molality of NH₃ in solution (mol kg⁻¹, calculated by
129 multiplying H_{NH_3} and p_{NH_3}), [NH₃(g)] is the equivalent molality of gaseous NH₃ in solution
130 (mol kg⁻¹, given by Equation 2), and [NH₄⁺(aq)] is the molality of NH₄⁺ in solution (mol kg⁻¹).
131 Equation 2 calculates [NH₃(g)], where p_{NH_3} is the partial pressure of NH₃ (atm), ρ_w is the
132 density of water (μg m⁻³), R is the gas constant (atm L mol⁻¹ K⁻¹), T is temperature (K), and
133 AWC is aerosol water content (μg m⁻³ air). Equation 3 calculates the last unknown term in
134 Equation 1, which is K_{a,NH_3}^* , the effective dissociation constant (where H_{NH_3} is the Henry's law
135 constant of NH₃ in mol kg⁻¹ atm⁻¹).

136 Direct measurements of aerosol pH are not available to test model predictions so the
137 partitioning of semi-volatile species that depend on pH, most commonly NH₃/NH₄⁺ and
138 HNO₃/NO₃⁻, is a key metric used to evaluate model performance (Pye et al., 2020).
139 ISORROPIA is used extensively for predictions of pH; however, in this study the measured and
140 ISORROPIA-predicted values of NH₃ partitioning ($\epsilon_{NH_3} = NH_3/(NH_3 + NH_4^+)$) did not always
141 agree well (Fig. S2). There were systematic differences in pH between the two methods (mean
142 pH difference = 0.6 pH units), and they were not correlated ($R^2 = 0.097$, not shown). The source

143 of the discrepancy in NH_3 partitioning (ISORROPIA modeled versus measurement-calculated) is
144 unknown, though it is not likely the result of an incorrect assumption of equilibrium (see the SI
145 and the companion paper Balasus et al. (2021) for more details).

146 Commonly, a reasonable estimate of measurement errors associated with the species of
147 interest are on the order of $15\% + 1 \text{ nmol m}^{-3}$ for online sampling methods (Murphy et al., 2017).
148 Utilizing this estimate in the extreme acidic case (ambient observed SO_4^{2-} and NO_3^- adjusted to +
149 $15\% + 1 \text{ nmol m}^{-3}$; NH_4^+ adjusted to $-15\% - 1 \text{ nmol m}^{-3}$) or non-acidic case (SO_4^{2-} and NO_3^-
150 adjusted down by $-15\% - 1 \text{ nmol m}^{-3}$ and NH_4^+ adjusted up by $+15\% + 1 \text{ nmol m}^{-3}$), the
151 uncertainty of aerosol pH was predicted to vary by 0.1 – 1 pH units (Murphy et al. 2017).
152 Similarly, Pye et al. (2020) reported that in cases for RH above 60%, deviations of the
153 ISORROPIA-predicted pH and the IUPAC-defined pH are less than one pH unit. The present
154 calculations have similar uncertainties in the pH calculations.

155

156 **3 Results and Discussion**

157 **3.1 Meteorological effect on pH**

158 As in many cities, the urban heat island effect in Baltimore evolves throughout the day,
159 with urban-rural temperature and RH gradients peaking at night (Battaglia et al., 2017).
160 Meteorological conditions at HMI demonstrate unique features associated with the land-water
161 transition. At night, the average temperature observed at HMI was close to conditions observed
162 in downtown Baltimore but transitioned to match the conditions at a nearby rural site during the
163 day (Fig. 1a). Overall, the range in average hourly temperatures at HMI was lower ($4.3 \text{ }^\circ\text{C}$; 22.5
164 $- 26.8 \text{ }^\circ\text{C}$) than the averages observed at either the downtown site (range $6.2 \text{ }^\circ\text{C}$; $22.8 - 29.0 \text{ }^\circ\text{C}$)
165 or the rural site (range $8.8 \text{ }^\circ\text{C}$; $17.5 - 26.3 \text{ }^\circ\text{C}$). Likewise, the average hourly RH profile at HMI

166 had a significantly smaller range (13.7%; 61.7 – 75.4%) than the RH profiles at the downtown
167 (range 22.1%; 53.2 – 75.3%) or rural sites (range 30.3%; 55.9 – 86.2%) (Fig. 1b). The
168 differences shown in Fig. 1 were due to the proximity of HMI to the Chesapeake Bay and have
169 several implications for aerosol pH, which will be discussed in detail below.

170 Due to the meteorological conditions discussed above, the diurnal profile of ALWC at
171 HMI was unique (Fig. 2a). Typical profiles of ALWC in the eastern US closely follow RH, with
172 minima in the afternoon and maxima at night or in the pre-dawn morning hours (Guo et al.,
173 2015; Battaglia et al., 2017). During OWLETS-2, ALWC did not show a distinct diurnal profile
174 that was correlated with RH. Instead, the highest median ALWC at HMI occurred between
175 12:00 – 14:00, (local time, LT; during the study this is UTC-4) (Fig. 2a). This daily peak in
176 ALWC coincided with a pronounced enhancement in aerosol NO_3^- , which is discussed in the
177 companion paper (Balasus et al., 2021). The partitioning of NH_3 , ϵ_{NH_3} , also showed a diurnal
178 profile that was unexpected (Fig. 2b). Due to the strong temperature dependence of vapor
179 pressure and equilibrium constants, NH_3 partitioning typically shifts towards the gas-phase
180 during the daytime (ϵ_{NH_3} increases) and shifts towards the aerosol phase at night (ϵ_{NH_3} decreases)
181 (Guo et al., 2017). The increase in gas-phase NH_3 emissions with increasing temperature can
182 also contribute to an elevated ϵ_{NH_3} during the daytime. The diurnal profile of ϵ_{NH_3} observed at
183 HMI did not follow temperature, as the median ϵ_{NH_3} peaked during the 06:00 – 08:00 LT, and
184 decreased slightly into the afternoon (Fig. 2b). This shows a shift of NH_3 partitioning towards
185 the condensed phase as daily temperatures peaked. This was enabled by the ALWC remaining
186 steady throughout the afternoon. Overall, the median ϵ_{NH_3} value for the entire OWLETS-2 study
187 was 0.915, showing NH_3 partitioning was shifted towards the gas-phase.

188 The diurnal profile of aerosol pH computed using the NH₃ partitioning method followed
189 a qualitatively similar pattern to prior studies (Battaglia et al. 2017), with maxima in the early
190 morning and minima in the afternoon; however, there was a much smaller amplitude in the
191 median hourly pH values (Fig. 3). The highest median pH value (1.97) was observed between
192 07:00 – 08:00 LT, while the lowest median pH (1.50) was observed between 16:00 – 17:00 LT.
193 For the entire study, there was only a ~1 pH unit difference between the 10th and 90th percentile
194 values (1.39 and 2.36, respectively). The relatively muted diurnal profile of aerosol pH was due
195 to the unique meteorology that resembled a nearby urban site at night and transitioned to match
196 the nearby rural site during the day. The companion paper shows the diurnal profiles of aerosol
197 inorganic composition (Balasus et al., 2021). Figures 2 and 3 are consistent with recent studies
198 that demonstrate the high sensitivity of pH to meteorological factors (Battaglia et al., 2017; Tao
199 & Murphy, 2019; Zheng et al., 2020). It is interesting to note that the ISORROPIA predictions
200 of aerosol pH yield a distinctly different diurnal profile than the pH predicted by NH₃
201 partitioning (Fig. S3). The difference in pH between the two methods peaked in the afternoon
202 between 12:00 – 14:00 LT, when particles were most acidic, and was a minimum in the early
203 morning when pH was highest (Fig. S3). The reason for these discrepancies are explored in the
204 discussion below.

205 Results suggest that pH was most sensitive to temperature changes at HMI during
206 OWLETS-2 (Fig. 4a). Across the full temperature range, the observed pH sensitivity to
207 temperature was -0.047 K⁻¹. A recent study contrasting pH in the southeast US and the North
208 China Plain found that temperature affects pH linearly at a rate of approximately -0.055 K⁻¹
209 (Zheng et al., 2020). A separate study from a Canadian observational network found that the
210 pH-temperature dependence is not linear, but changes with temperature (Tao and Murphy, 2019;

211 Tao, 2020). Over the range of conditions observed during OWLETS-2, Tao (2020) computed a
212 pH sensitivity to temperature of approximately -0.045 K^{-1} to -0.055 K^{-1} . In a previous study, the
213 pH sensitivity to temperature in Baltimore was -0.048 K^{-1} , though this was calculated for
214 conditions of constant atmospheric composition (Battaglia et al., 2017). While the present
215 results share consistencies with these studies, the results in Fig. 4a suggest important differences,
216 as well. An increase in pH was observed with increasing temperature for conditions below 293
217 K (n=156). In the companion paper, NH_3 concentrations dramatically increased with
218 temperature $< 293 \text{ K}$ but exhibited a much weaker dependence on temperature for conditions $>$
219 293 K (Balasus et al., 2021). Under the warmer conditions, the pH relationship with temperature
220 was linear during OWLETS-2, with a sensitivity of -0.085 K^{-1} (Fig. 4a). The results in Fig. 4a
221 are consistent with Tao (2020), as they demonstrate the offsetting responses of pH to temperature
222 through effects on NH_3 emissions and partitioning.

223 These results contribute to the growing body of work demonstrating the importance of
224 temperature to aerosol pH. Collectively, these studies suggest that the sensitivity of pH to
225 temperature is constrained between -0.045 K^{-1} and -0.085 K^{-1} , although the present results
226 illustrate circumstances where a positive relationship between temperature and pH can exist, as
227 well. It is notable that similar $\Delta\text{pH}/\Delta\text{T}$ values are observed across a range of locations and for
228 variable data sets that include monthly averages of long-term observations (Tao and Murphy,
229 2019) and 20-min measurements made over a period of weeks (presented here).

230 Aerosol pH was not strongly affected by ALWC over the range of conditions observed
231 during OWLETS-2, except at ALWC below $1 \mu\text{g m}^{-3}$ (Fig. 4b). At the lowest ALWC levels, the
232 increase in pH occurs because of the diluting effect of water, however, at ALWC above $1 \mu\text{g m}^{-3}$,
233 other factors appear to be more important (e.g., temperature). ALWC was recently identified as

234 the most significant contributor to regional pH differences (Zheng et al., 2020). In that study, the
235 pH-ALWC relationship was highly non-linear, with the greatest sensitivity calculated at ALWC
236 at levels $< 25 \mu\text{g m}^{-3}$, conditions corresponding to all the OWLETS-2 observations. Tao (2020)
237 found that pH is extremely sensitive to RH, presumed to be a surrogate for ALWC, when RH
238 was $< 20\%$ or $\text{RH} > 80\%$; however, pH was quite insensitive to RH variations in the region of
239 $20\% < \text{RH} < 80\%$. Approximately 25% (208 out of 875) of RH values during OWLETS-2 were
240 above 80%, yet no increase in pH was observed at the highest ALWC, suggesting that other
241 factors were offsetting the diluting effect of water as ALWC increased. It is interesting to note
242 that ISORROPIA predicts a stronger effect of ALWC on pH, with the diluting effect apparent as
243 pH increases with increasing ALWC. A combination of particle mass loading, aerosol
244 composition, and ambient RH are responsible for the variations in ALWC.

245 The result shown in Fig. 4b is somewhat surprising because NH_3 partitioning was quite
246 sensitive to ALWC (Fig. 5); the relatively invariant aerosol pH is unexpected given the increase
247 in NH_3 uptake in the presence of ALWC. With increasing NH_3 uptake in the presence of, and
248 concurrent with, the increased ALWC, it would be anticipated that aerosol pH would become
249 more basic both through the reaction of NH_3 to form NH_4^+ and due to the dilution effect of liquid
250 water. However, the results of Figures 4 and 5 reveal that despite both the increase in NH_3
251 uptake and increase in ALWC, aerosol pH remains relatively unchanged, with only a 0.5 pH unit
252 change at the highest values of ALWC. NH_3 partitioning shifted towards the condensed phase
253 (ϵ_{NH_3} decreased) at increasing ALWC, consistent with the results of Nenes et al. (2020). ϵ_{NH_3}
254 was more sensitive to ALWC than it was to either temp or RH (Fig. S5). This result shows the
255 importance that ALWC can have on $\text{PM}_{2.5}$ mass concentrations, as water serves as an important
256 medium enhancing the condensation of organic and inorganic water-soluble species (Carlton et

257 al., 2018; El-Sayed et al., 2016). Fig. 5 demonstrates the importance of ALWC in changing the
258 dry deposition of reactive nitrogen species. Nenes et al. (2021) predicts that NH_3 and HNO_3 dry
259 deposition rates will both be high under the conditions observed during OWLETS-2 (i.e., ALWC
260 $< 10 \mu\text{g m}^{-3}$ and $\text{pH} \sim 1.5$). This is also consistent with a modeling study showing increased dry
261 deposition of reactive nitrogen in coastal regions, including the OWLETS-2 study domain
262 (Loughner et al., 2016).

263

264 3.2 Composition Effects on Aerosol pH

265 In contrast to meteorological factors, aerosol composition did not have a major effect on
266 pH variability during OWLETS-2. Consistent with prior studies, neither the sulfate
267 concentration nor the $\text{NH}_4^+:\text{SO}_4^{2-}$ molar ratio contributed significantly to pH variability (Weber
268 et al., 2016; Hennigan et al., 2015). Fig. 4c shows that pH was also relatively insensitive to the
269 Tot- NH_3 concentration, in agreement with the results from other locations (Zheng et al., 2020;
270 Tao, 2020; Weber et al., 2016). While the predictions of ISORROPIA generally did not capture
271 the trends between pH and the meteorological factors, it is interesting to note that ISORROPIA
272 predicts that pH is relatively insensitive to Tot- NH_3 , as well, except at the highest concentrations
273 (Fig. S4).

274 Composition and concentration differences between HMI and the urban and rural sites
275 are analyzed in more detail in the companion paper (Balasus et al., 2021). In the companion
276 paper, episodic NH_3 events that derived from dairy, poultry, and industrial sources were
277 characterized (Balasus et al., 2021). For the events with complete aerosol composition and
278 meteorology data (8 out of 11 NH_3 events total), mean and median aerosol pH (2.00 and 1.96,
279 respectively) were only moderately higher than the study mean and median pH values (1.85 and

280 1.83, respectively); this difference is not statistically significant at the 95% confidence interval.
281 This includes an aerosol pH of 1.92 at the peak NH₃ concentration observed during the entire
282 study (19.3 μg m⁻³), an event influenced by industrial emissions near downtown Baltimore
283 (Balasus et al., 2021). Together, the results suggest that pH may be more affected by the
284 proximity of the HMI site to the Chesapeake Bay than it was to regional agricultural NH₃
285 emissions, or to episodic NH₃ events from local industrial sources.

286

287 **3.3 Case Study: Effect of NVCs on pH**

288 NVCs affect thermodynamic predictions of NH₃ partitioning and thus, pH (Guo et al.,
289 2018; Vasilakos et al., 2018). Seawater is alkaline and primary marine emissions contain high
290 concentrations of NVCs (O'Dowd & De Leeuw, 2007). Marine aerosols rapidly acidify,
291 typically in seconds or minutes, though the timescale depends upon particle size (Angle et al.,
292 2021; Pszenny et al., 2004). Studies have examined the acidity of sea spray aerosols and their
293 evolution but none, to our knowledge, have done so in a polluted urban environment. The
294 OWLETS-2 study offered a unique opportunity to analyze the pH of primary marine particles
295 emitted within several km of a large urban area. The Chesapeake Bay is brackish, with
296 increasing salinity moving down the bay towards the Atlantic Ocean (Pritchard, 1952). Near the
297 OWLETS-2 measurement site at HMI, salinity is variable but average conditions are ~5 g kg⁻¹
298 (www.chesapeakebay.net, last accessed 20-November 2020). This is about a factor of seven
299 lower than typical seawater, but shows the potential for primary emissions to contribute salts that
300 could impact aerosol pH at HMI.

301 Elevated concentrations of Na⁺ and Cl⁻ in PM_{2.5} were infrequently observed during
302 OWLETS-2, with one notable 36-hour period showing evidence of primary marine impact. Na⁺

303 and Cl^- were well-correlated ($R^2 = 0.78$) from 11-June to 13-June, a period that coincided with
304 the highest concentrations of both species (Fig. 6 and Fig. 7). It is noteworthy that wind speeds
305 were not elevated during this time (average winds = 3.1 m s^{-1} compared to campaign-average
306 wind speeds of 2.9 m s^{-1}); longer-term measurements would be needed to characterize factors
307 driving the primary bay emissions. During this event, the pH calculation using NH_3 partitioning
308 suggests that the primary marine emissions had a minimal effect on aerosol pH. The average pH
309 during this period was 1.98, which was only slightly higher than the average for the entire study
310 (1.85). Further, as the total $\text{Na}^+ + \text{Cl}^-$ concentration increased by more than an order of
311 magnitude, from $0.05 \mu\text{g m}^{-3}$ around 18:00 LT on 11 June to $0.9 \mu\text{g m}^{-3}$ at 09:00 LT on 12 June,
312 the pH only increased by 0.1 pH unit during the same period (Fig. 6). Gas-phase NH_3 data were
313 not available for the entire NaCl event, so pH calculations were limited to the first ~20 hours.

314 The pH predictions from ISORROPIA during this period display a more significant effect
315 on aerosol pH. The average pH predicted by ISORROPIA is 3.08, which is 0.7 pH units higher
316 than the study average from ISORROPIA. Further, while the pH calculated using NH_3
317 partitioning is insensitive to Na^+ and Cl^- , ISORROPIA predicts a rise of 1.4 pH units as Na^+ and
318 Cl^- increase (Figure 6). The NH_3 partitioning predicted by ISORROPIA deviates from the
319 observations during this event ($r = -0.19$, Fig. S6). The most likely explanation for this behavior
320 is different chemical compositions of the coarse- and fine-mode particles. Fresh marine
321 emissions acidify quickly, and evidence was found for chemical processing of NaCl. HNO_3
322 displacement of HCl is a well-known phenomenon in sea salt particles (Brimblecombe & Clegg,
323 1988). $\text{Cl}^-:\text{Na}^+$ ratios slightly above unity were observed when aerosol nitrate concentrations
324 were low, and below unity when nitrate concentrations were elevated (Fig. 7). Nitrate formation,
325 including HNO_3 uptake to sea salt, is highly sensitive to pH (Kakavas et al., 2021; Vasilakos et

326 al., 2018). Nitrate (along with Na^+ and Cl^-) are direct inputs to ISORROPIA, suggesting that the
327 pH trend in Fig. 6 is due to the increased influence of coarse-mode particles. The PILS inlet was
328 equipped with a 2.5 μm cut-point cyclone (URG-2000-30-EH, URG Corp.), which allows some
329 penetration of particles with $d_p < 4.5 \mu\text{m}$ ([http://www.urgcorp.com/products/inlets/teflon-coated-](http://www.urgcorp.com/products/inlets/teflon-coated-aluminum-cyclones/urg-2000-30eh)
330 [aluminum-cyclones/urg-2000-30eh](http://www.urgcorp.com/products/inlets/teflon-coated-aluminum-cyclones/urg-2000-30eh), last accessed 29 January 2021). Likewise, primary sea salt
331 emissions often exhibit a size distribution tail that extends below 2.5 μm (Feng et al., 2017).

332 The above analysis identifies limitations computing aerosol pH with both approaches and
333 highlights opportunities to use complementary information from each to inform factors driving
334 aerosol pH. ISORROPIA's assumption of an internally mixed aerosol distribution cannot be
335 applied to predict pH in this system (Fountoukis and Nenes, 2007). However, it does provide
336 insight into the likely presence of coarse mode particles with pH significantly higher than the
337 fine mode. Conversely, Na^+ , Cl^- and NO_3^- are not direct inputs into the pH calculation using
338 NH_3 partitioning, though they are used to compute aerosol liquid water, which is an input in the
339 pH calculation (Zheng et al., 2020). These NVCs have been shown to have sometimes
340 significant effects on the ratios of ammonium-to-sulfate, which could lead to inconsistencies in
341 the calculation of aerosol pH when considered in the ALWC calculation only (Guo et al. 2015).
342 NH_4^+ resides predominantly in the fine mode (Seinfeld & Pandis, 2016), so the partitioning
343 approach is unlikely to capture the acidity of the coarse mode or fine-mode particles in the tail of
344 the distribution of primary emissions that may be externally mixed with secondary particles, such
345 as dust or sea salt. This may lead to underestimates of NVC effects on aerosol pH using the
346 partitioning approach. The combined information from both methods suggests that aerosols
347 sampled at HMI during the NaCl event were characterized by a strong size-dependent pH
348 gradient, with fine-mode particles more acidic (pH ~2) than the coarse mode (pH up to 4.5).

349 Estimates of pH derived from size-segregated aerosol composition measurements have observed
350 the same phenomenon (Angle et al., 2021; Fang et al., 2017; Kakavas et al., 2021; Keene et al.,
351 2002).

352

353 **4 Conclusions**

354 There is growing recognition of the importance of aerosol pH affecting atmospheric
355 processes relevant to public health and ecosystems (Fang et al., 2017; Nenes et al., 2021).
356 Observations of spatial and temporal variations in pH are needed so that the factors that control
357 pH and contribute to variability in different environments can be fully understood. This study is
358 unique as it represents the first characterization of aerosol pH at a land-water transition site near
359 a large urban area. Baltimore, MD, is impacted by regional agricultural emissions and by
360 industrial point-source emissions of NH_3 . The companion paper examines the sources of
361 episodic NH_3 events and the associated effects on aerosol composition (Balasus et al., 2021).
362 Although average and peak NH_3 concentrations during this study were significantly higher than a
363 nearby inland site, the effects on aerosol pH appear relatively insignificant, as pH during the
364 peak events was only ~ 0.1 pH unit higher than non-event periods. This finding is consistent with
365 studies at other locations that show aerosol pH is often insensitive to Tot- NH_3 and to the aerosol
366 $\text{NH}_4:\text{SO}_4$ ratio (Weber et al., 2016; Zheng et al., 2020; Tao and Murphy, 2019).

367 The unique characteristics of the OWLETS-2 study and measurement locations also
368 offered insight into the composition and meteorological influences on aerosol pH. In the
369 companion paper, the composition effects were shown to be muted in comparison to the
370 meteorological effects (Balasus et al., 2021). It was shown that the unique diurnal profiles,
371 particularly in ALWC (which did not correlate with RH) and ϵ_{NH_3} (which did not correlate with

372 T) resulted in meteorological factors, notably temperature, having the most important influence
373 on aerosol pH. Across the full temperature range of the study, the observed pH sensitivity to
374 temperature was -0.047 K^{-1} , with increases in sensitivity up to -0.085 K^{-1} when the temperature
375 was $> 293 \text{ K}$. The sensitivity of aerosol pH shown here is in good agreement with previous
376 studies in the Baltimore region and beyond, *e.g.* Toronto (Tao and Murphy, 2019; Battaglia et al.
377 2017). Conversely, aerosol pH was not strongly affected by ALWC during the OWLETS-2
378 study, except when ALWC was below $1 \mu\text{g m}^{-3}$, in contrast to the results of Zheng et al. (2020).
379 These results of Zheng et al. (2020) in identifying ALWC as the most important factor driving
380 aerosol pH variability were derived from the results of studies in multiple locations, including
381 bulk aqueous solutions. However, this analysis suggests that the factors that drive aerosol pH
382 variability may exhibit important site-to-site differences that must be considered before
383 generalizations are applied.

384 A case study of the NVC effect on aerosol pH had significantly different outcomes
385 depending on the method for calculating pH. ISORROPIA predicted a pH increase of $\sim 1.4 \text{ pH}$
386 units during an event with primary aerosol emissions from the Chesapeake Bay, while the pH
387 calculation using NH_3 partitioning predicted a much less significant effect ($\sim 0.1 \text{ pH}$ unit). This
388 difference is attributed to the likely presence of externally mixed particles during the events,
389 which may include primary marine emissions elevated in NVCs. Bougiatioti et al. (2016)
390 evaluated aerosol pH at a remote site in the Mediterranean, where samples with a marine origin
391 demonstrated vastly different pH between fine (avg. pH = 0.4) and coarse mode (average pH =
392 7.3) particles. Similarly, Keene et al. (2002) demonstrated the effect of marine aerosol size
393 distribution on aerosol pH, with fine mode particles predicted to reside in the range of 1-2, with
394 super- μm particles to reside in the range of 3-4, consistent with the current results. Hence, a

395 limitation of this study is the lack of size-resolved aerosol composition measurements. This
396 study underscores the need to evaluate assumptions of internally mixed aerosols when applying
397 pH calculations, which may be a critical factor in overestimating the effects of NVCs on pH.
398 Models with size-resolved aerosol composition may be required to capture this effect across
399 scales in future studies (Kakavas et al., 2021).

400

401 **Data Availability**

402 Data are available at <https://www-air.larc.nasa.gov/cgi-bin/ArcView/owlets.2018>.

403

404 **Supplement**

405 **Supplemental Information is available for this article at:**

406

407 **Acknowledgements**

408 Annmarie G. Carlton and Christopher J. Hennigan acknowledge funding from the National Science
409 Foundation, AGS-1719252 and AGS-1719245. Ruben Delgado and Vanessa Caicedo acknowledge
410 support by the Maryland Department of the Environment (contract no. U00P8400651). Nicholas Balasus
411 and Katherine Ball received support through the NOAA Office of Education, Educational Partnership
412 Program with Minority Serving Institutions (EPP/MSI) and the Cooperative Science Center for Earth
413 System Sciences and Remote Sensing Technologies (grant no. NA16SEC4810008).

414 **Author Contributions**

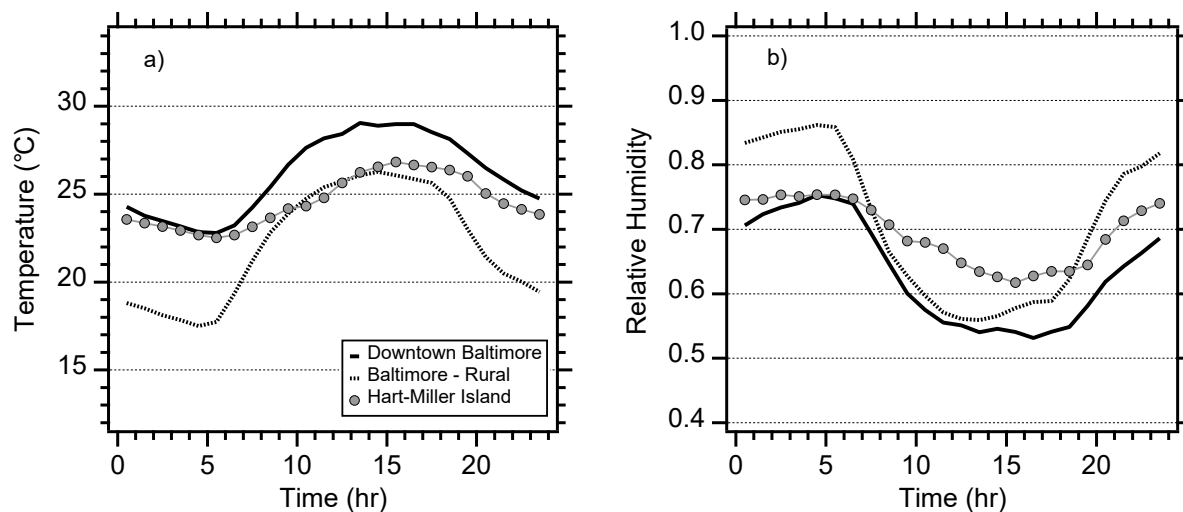
415 CH, AC, and RD conceived the analysis and study participation. MB, NB, and KB collected and
416 analyzed the PILS-IC and NH₃ data. NB, MB, and CH conducted the thermodynamic modeling
417 analyses. VC and AC provided analytical input and interpretation. NB, CH, KB, and MB wrote
418 the manuscript. All authors provided feedback and revisions to the manuscript.

419

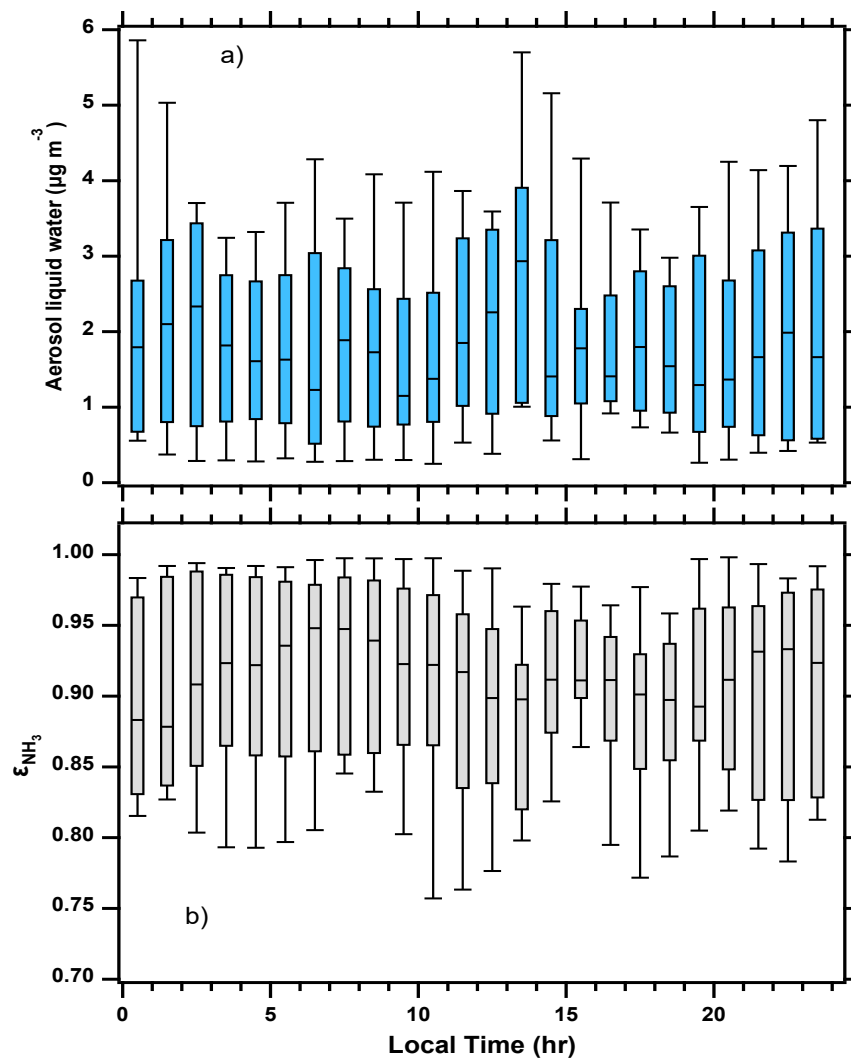
420 **Competing Interests**

421 The authors declare they have no conflict of interest.

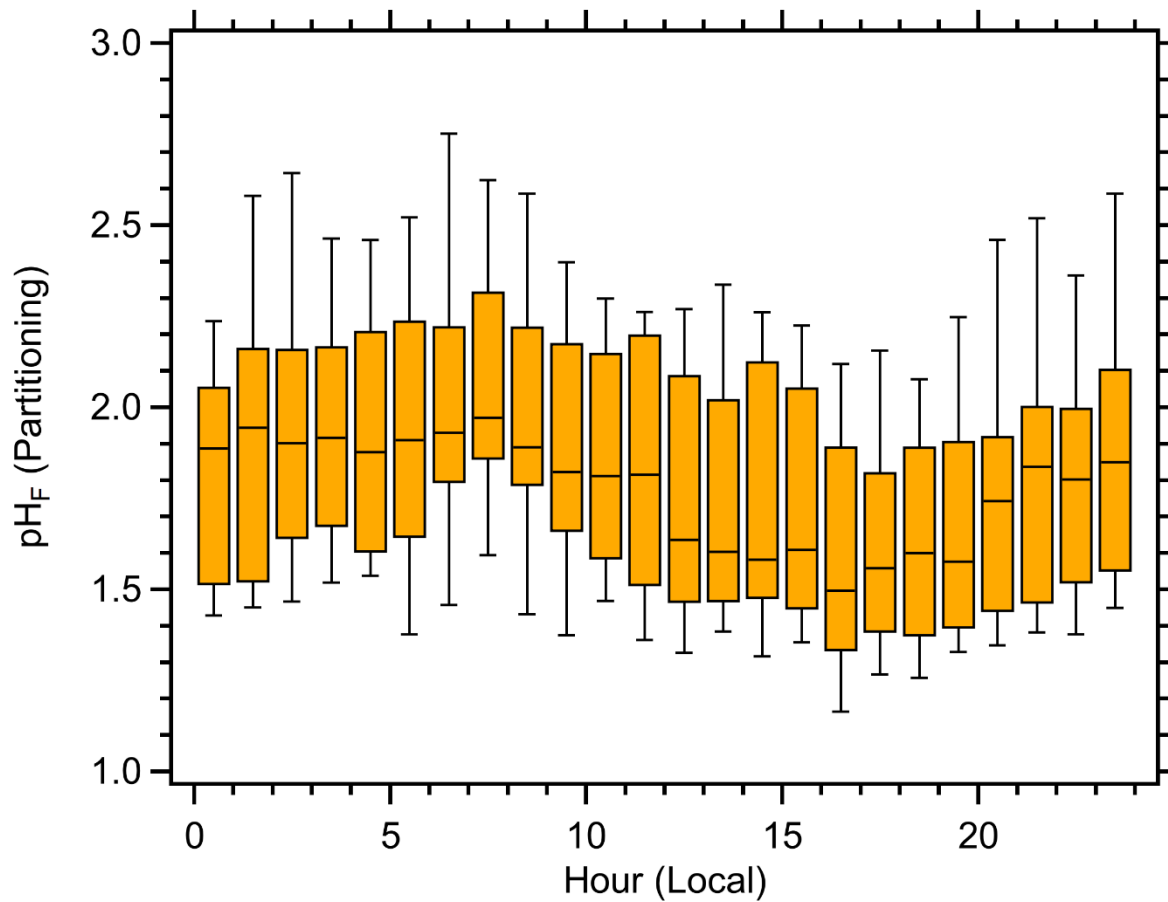
422 **Figures**
423



424
425 **Figure 1:** Diurnal profiles of (a) temperature and (b) relative humidity at three sites during the
426 OWLETS-2 study. Hart-Miller Island (HMI) is a land-water transition site and was the location
427 of aerosol composition and gas-phase measurements during the campaign. Temperatures at HMI
428 resembled the downtown location during the night but showed characteristics of the rural site
429 during the day. RH at HMI was between the urban and rural sites at night but was elevated
430 during the daytime due to the Chesapeake Bay.

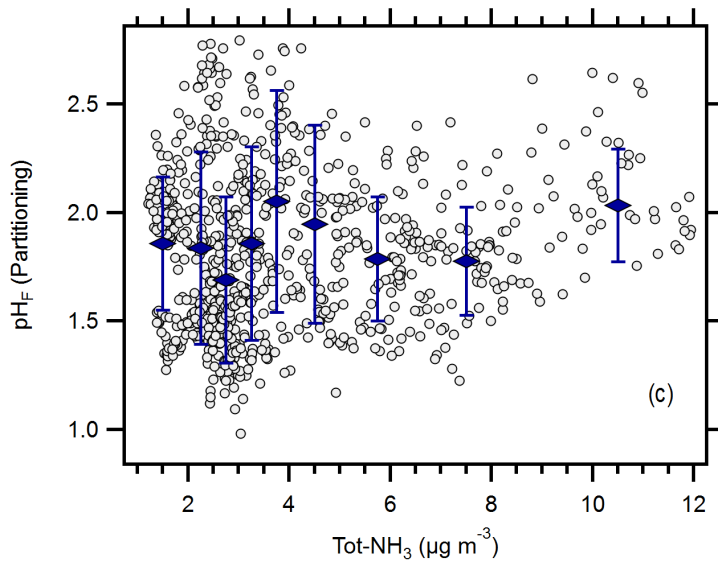
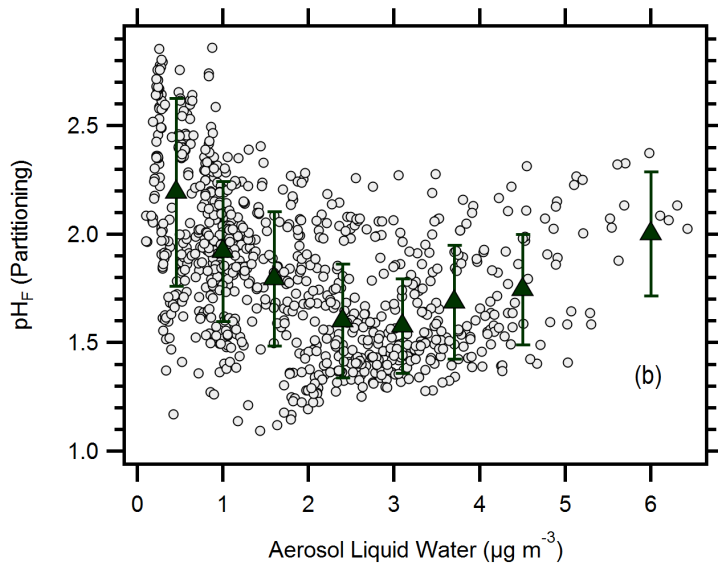
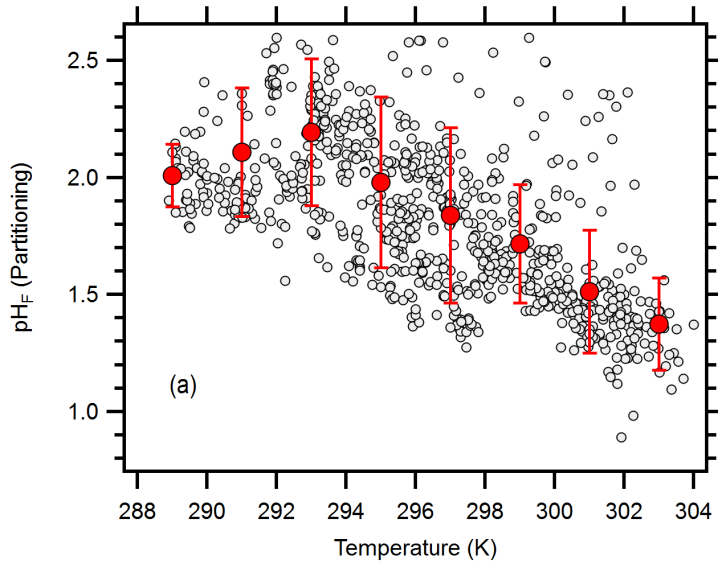


431
 432 **Figure 2:** Box plots of (a) aerosol liquid water and (b) ϵ_{NH_3} ($\epsilon_{NH_3} = NH_3(g)/(NH_3(g) + NH_4^+(aq))$)
 433 during the OWLETS-2 study. The statistics shown are the median, quartiles, 10th and 90th
 434 percentiles.

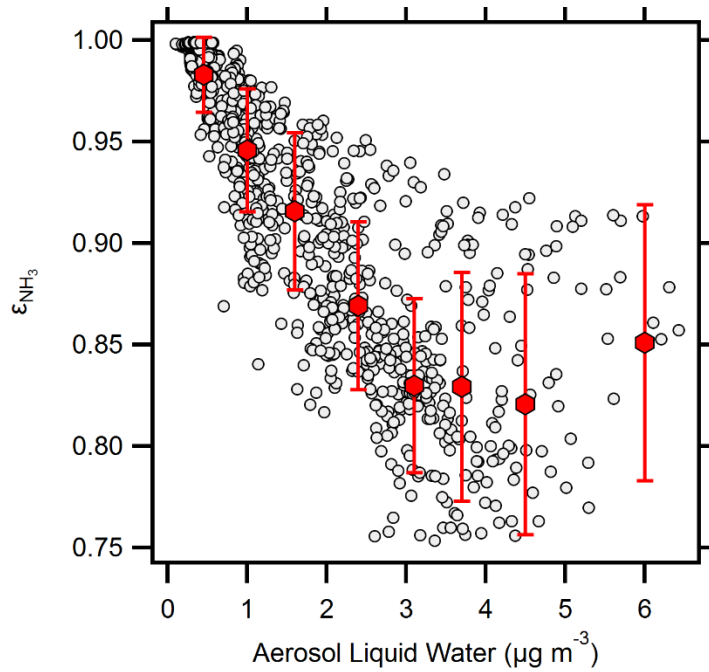


435

436 **Figure 3:** Box plot of the aerosol pH diurnal profile calculated using the NH₃ partitioning
 437 method of at Hart-Miller Island during OWLETS-2. The statistics shown are the median,
 438 quartiles, 10th and 90th percentiles.



440 **Figure 4:** Relationship between aerosol pH and (a) temperature, (b) aerosol liquid water, and (c)
441 total NH₃ (Tot-NH₃ = NH₃ + NH₄⁺). Symbols represent mean values while error bars represent
442 standard deviations; bins were limited to a maximum of 160 points per bin.



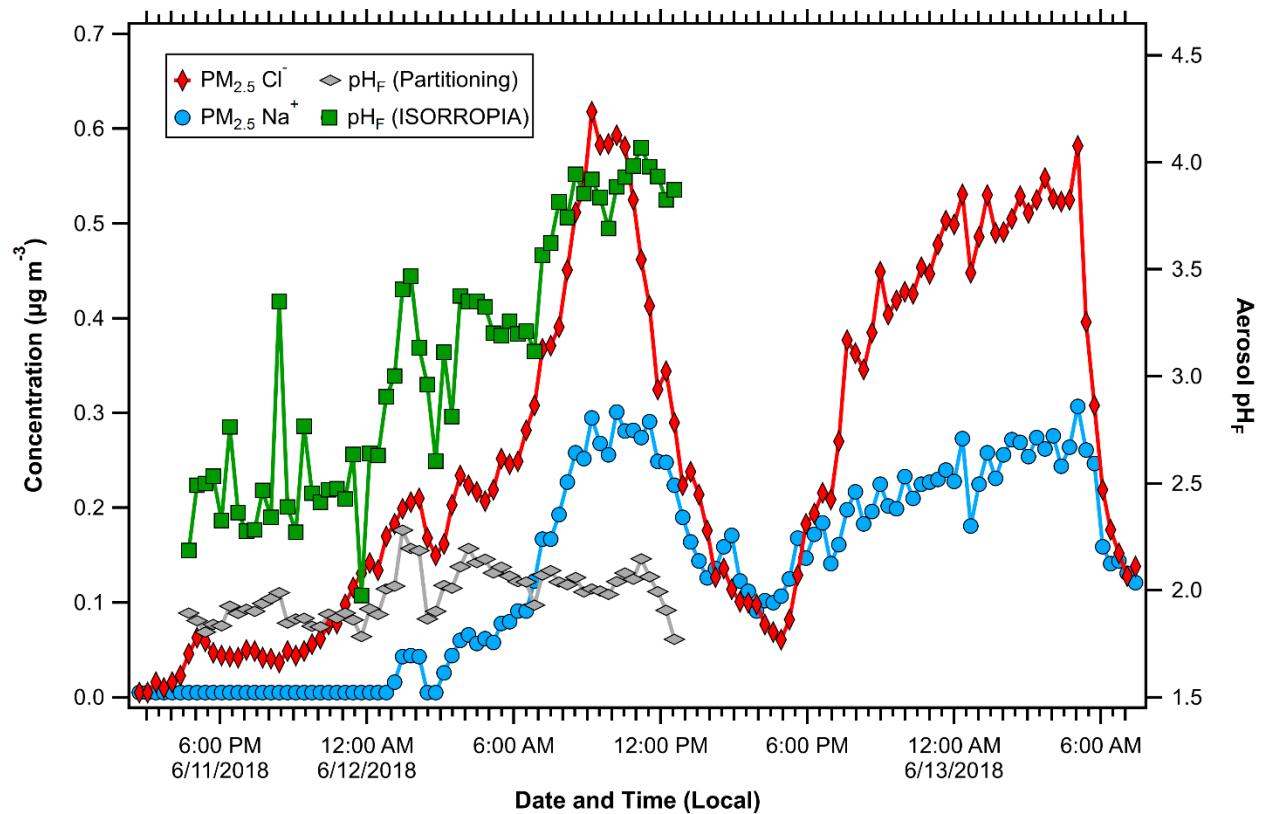
443

444 **Figure 5:** Relationship between NH_3 partitioning ($\epsilon_{\text{NH}_3} = \text{NH}_3/(\text{NH}_3 + \text{NH}_4^+)$) and aerosol liquid

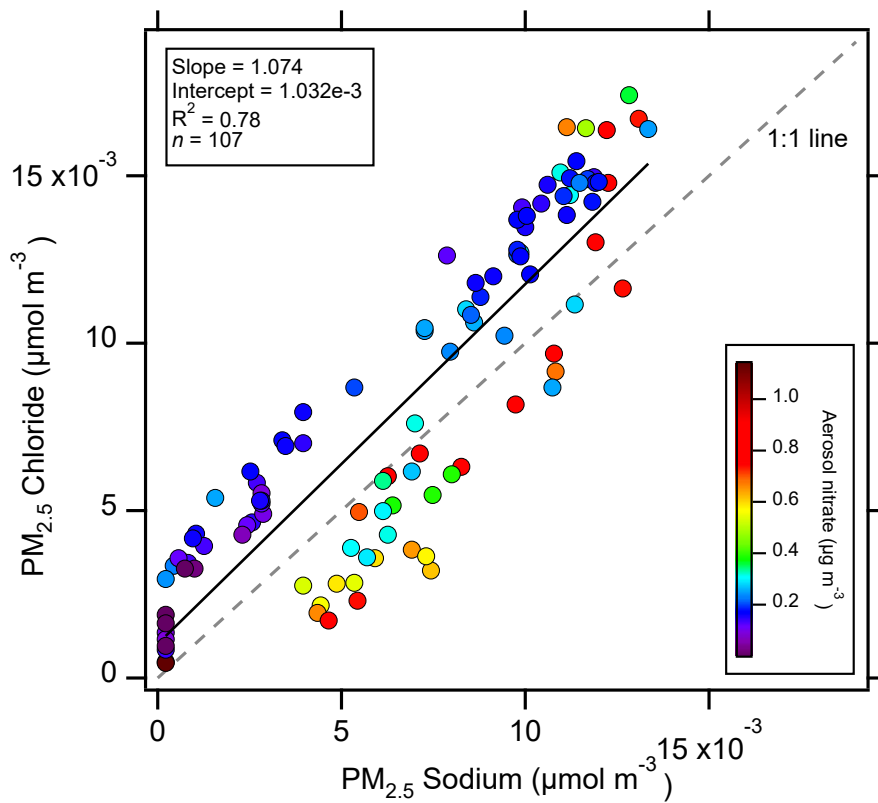
445 water. Symbols represent mean values while error bars represent standard deviations; bins were

446 limited to a maximum of 160 points per bin.

447



448
 449 **Figure 6:** Concentrations of $\text{PM}_{2.5} \text{Na}^+$ and Cl^- during a period with primary Chesapeake Bay
 450 emissions. Aerosol pH calculated by NH_3 partitioning and ISORROPIA show different
 451 behaviors, suggesting the aerosol distribution was externally mixed during this time.



452

453 **Figure 7:** Correlation between $\text{PM}_{2.5} \text{Na}^+$ and Cl^- during the event shown in Figure 6. Lower
 454 $\text{Cl}^-:\text{Na}^+$ ratios were observed at higher NO_3^- concentrations, suggesting HNO_3 uptake displaced
 455 HCl .

References

- 456
457
458 Angle, K. J., Crocker, D. R., Simpson, R. M. C., Mayer, K. J., Garofalo, L. A., Moore, A. N., Garcia, S.
459 L. M., Or, V. W., Srinivasan, S., Farhan, M., Sauer, J. S., Lee, C., Pothier, M. A., Farmer, D. K.,
460 Martz, T. R., Bertram, T. H., Cappa, C. D., Prather, K. A., & Grassian, V. H. (2021). Acidity
461 across the interface from the ocean surface to sea spray aerosol. *Proceedings of the National*
462 *Academy of Sciences of the United States of America*, 118(2), Article e2018397118.
463 <https://doi.org/10.1073/pnas.2018397118>
- 464 Balasus, N., Battaglia Jr, M. A., Ball, K., Caicedo, V., Delgado, R., Carlton, A. G., & Hennigan, C. J.
465 (2021). Urban aerosol chemistry at a land–water transition site during summer – Part 1: Impact of
466 agricultural and industrial ammonia emissions. *Atmos. Chem. Phys.*, 21(17), 13051-13065.
467 <https://doi.org/10.5194/acp-21-13051-2021>
- 468 Battaglia Jr, M. A., Weber, R. J., Nenes, A., & Hennigan, C. J. (2019). Effects of water-soluble organic
469 carbon on aerosol pH. *Atmos. Chem. Phys.*, 19(23), 14607-14620. [https://doi.org/10.5194/acp-19-](https://doi.org/10.5194/acp-19-14607-2019)
470 [14607-2019](https://doi.org/10.5194/acp-19-14607-2019)
- 471 Battaglia, M. A., Douglas, S., & Hennigan, C. J. (2017). Effect of the Urban Heat Island on Aerosol pH.
472 *Environ. Sci. Technol.*, 51(22), 13095-13103. <https://doi.org/10.1021/acs.est.7b02786>
- 473 Bougiatioti, A., Nikolaou, P., Stavroulas, I., Kouvarakis, G., Weber, R., Nenes, A., Kanakidou, M., &
474 Mihalopoulos, N. (2016). Particle water and pH in the eastern Mediterranean: source variability
475 and implications for nutrient availability. *Atmos. Chem. Phys.*, 16(7), 4579-4591.
476 <https://doi.org/10.5194/acp-16-4579-2016>
- 477 Boyer, H. C., Gorkowski, K., & Sullivan, R. C. (2020). In Situ pH Measurements of Individual Levitated
478 Microdroplets Using Aerosol Optical Tweezers. *Analytical Chemistry*, 92(1), 1089-1096.
479 <https://doi.org/10.1021/acs.analchem.9b04152>
- 480 Brimblecombe, P., & Clegg, S. L. (1988). The Solubility and Behavior of Acid Gases in the Marine
481 Aerosol. *Journal of Atmospheric Chemistry*, 7(1), 1-18. <https://doi.org/10.1007/bf00048251>
- 482 Carlton, A. M. G., Pye, H. O. T., Baker, K. R., & Hennigan, C. J. (2018). Additional benefits of federal
483 air quality rules: model estimates of controllable biogenic secondary organic aerosol.
484 *Environmental Science & Technology*. <https://doi.org/10.1021/acs.est.8b01869>
- 485 Craig, R. L., Peterson, P. K., Nandy, L., Lei, Z., Hossain, M. A., Camarena, S., Dodson, R. A., Cook, R.
486 D., Dutcher, C. S., & Ault, A. P. (2018). Direct Determination of Aerosol pH: Size-Resolved
487 Measurements of Submicrometer and Supermicrometer Aqueous Particles. *Analytical Chemistry*,
488 90(19), 11232-11239. <https://doi.org/10.1021/acs.analchem.8b00586>
- 489 El-Sayed, M. M. H., Amenumey, D., & Hennigan, C. J. (2016). Drying-Induced Evaporation of
490 Secondary Organic Aerosol during Summer. *Environmental Science & Technology*, 50(7), 3626-
491 3633. <https://doi.org/10.1021/acs.est.5b06002>
- 492 Fang, T., Guo, H. Y., Zeng, L. H., Verma, V., Nenes, A., & Weber, R. J. (2017). Highly Acidic Ambient
493 Particles, Soluble Metals, and Oxidative Potential: A Link between Sulfate and Aerosol Toxicity.
494 *Environmental Science & Technology*, 51(5), 2611-2620. <https://doi.org/10.1021/acs.est.6b06151>

- 495 Feng, L., Shen, H., Zhu, Y., Gao, H., & Yao, X. (2017). Insight into Generation and Evolution of Sea-Salt
496 Aerosols from Field Measurements in Diversified Marine and Coastal Atmospheres. *Scientific*
497 *Reports*, 7, Article 41260. <https://doi.org/10.1038/srep41260>
- 498 Fountoukis, C., & Nenes, A. (2007). ISORROPIA II: a computationally efficient thermodynamic
499 equilibrium model for K^+ - Ca^{2+} - Mg^{2+} - NH_4^+ - Na^+ - SO_4^{2-} - NO_3^- - Cl^- - H_2O aerosols. *Atmos. Chem.*
500 *Phys.*, 7(17), 4639-4659. <https://doi.org/10.5194/acp-7-4639-2007>
- 501 Guo, H., Liu, J., Froyd, K. D., Roberts, J. M., Veres, P. R., Hayes, P. L., Jimenez, J. L., Nenes, A., &
502 Weber, R. J. (2017). Fine particle pH and gas-particle phase partitioning of inorganic species in
503 Pasadena, California, during the 2010 CalNex campaign. *Atmos. Chem. Phys.*, 17(9), 5703-5719.
504 <https://doi.org/10.5194/acp-17-5703-2017>
- 505 Guo, H., Nenes, A., & Weber, R. J. (2018). The underappreciated role of nonvolatile cations in aerosol
506 ammonium-sulfate molar ratios. *Atmos. Chem. Phys.*, 18(23), 17307-17323.
507 <https://doi.org/10.5194/acp-18-17307-2018>
- 508 Guo, H., Xu, L., Bougiatioti, A., Cerully, K. M., Capps, S. L., Hite, J. R., Carlton, A. G., Lee, S. H.,
509 Bergin, M. H., Ng, N. L., Nenes, A., & Weber, R. J. (2015). Fine-particle water and pH in the
510 southeastern United States. *Atmos. Chem. Phys.*, 15(9), 5211-5228. <https://doi.org/10.5194/acp-15-5211-2015>
- 512 He, H., Stehr, J. W., Hains, J. C., Krask, D. J., Doddridge, B. G., Vinnikov, K. Y., Canty, T. P., Hosley,
513 K. M., Salawitch, R. J., Worden, H. M., & Dickerson, R. R. (2013). Trends in emissions and
514 concentrations of air pollutants in the lower troposphere in the Baltimore/Washington airshed
515 from 1997 to 2011. *Atmospheric Chemistry and Physics*, 13(15), 7859-7874.
516 <https://doi.org/10.5194/acp-13-7859-2013>
- 517 Hennigan, C. J., Izumi, J., Sullivan, A. P., Weber, R. J., & Nenes, A. (2015). A critical evaluation of
518 proxy methods used to estimate the acidity of atmospheric particles. *Atmos. Chem. Phys.*, 15(5),
519 2775-2790. <https://doi.org/10.5194/acp-15-2775-2015>
- 520 Jang, M., Sun, S., Winslow, R., Han, S., & Yu, Z. (2020). In situ aerosol acidity measurements using a
521 UV-Visible micro-spectrometer and its application to the ambient air. *Aerosol Science and*
522 *Technology*, 54(4), 446-461. <https://doi.org/10.1080/02786826.2020.1711510>
- 523 Kakavas, S., Patoulias, D., Zakoura, M., Nenes, A., & Pandis, S. N. (2021). Size-resolved aerosol pH
524 over Europe during summer. *Atmos. Chem. Phys.*, 21(2), 799-811. <https://doi.org/10.5194/acp-21-799-2021>
- 526 Kanakidou, M., Myriokefalitakis, S., Daskalakis, N., Fanourgakis, G., Nenes, A., Baker, A. R., Tsigaridis,
527 K., & Mihalopoulos, N. (2016). Past, Present, and Future Atmospheric Nitrogen Deposition. *J.*
528 *Atmos. Sci.*, 73(5), 2039-2047. <https://doi.org/10.1175/jas-d-15-0278.1>
- 529 Keene, W. C., Pszenny, A. A. P., Maben, J. R., & Sander, R. (2002). Variation of marine aerosol acidity
530 with particle size. *Geophysical Research Letters*, 29(7), Article 1101.
531 <https://doi.org/10.1029/2001gl013881>
- 532 Keene, W. C., Pszenny, A. A. P., Maben, J. R., Stevenson, E., & Wall, A. (2004). Closure evaluation of
533 size-resolved aerosol pH in the New England coastal atmosphere during summer. *J. Geophys.*
534 *Res.-Atmos.*, 109(D23), D23307, Article D23307. <https://doi.org/10.1029/2004jd004801>

- 535 Loughner, C. P., Tzortziou, M., Follette-Cook, M., Pickering, K. E., Goldberg, D., Satam, C.,
536 Weinheimer, A., Crawford, J. H., Knapp, D. J., Montzka, D. D., Diskin, G. S., & Dickerson, R.
537 R. (2014). Impact of Bay-Breeze Circulations on Surface Air Quality and Boundary Layer
538 Export. *Journal of Applied Meteorology and Climatology*, 53(7), 1697-1713.
539 <https://doi.org/10.1175/jamc-d-13-0323.1>
- 540 Loughner, C. P., Tzortziou, M., Shroder, S., & Pickering, K. E. (2016). Enhanced dry deposition of
541 nitrogen pollution near coastlines: A case study covering the Chesapeake Bay estuary and
542 Atlantic Ocean coastline. *Journal of Geophysical Research-Atmospheres*, 121(23), 14221-14238.
543 <https://doi.org/10.1002/2016jd025571>
- 544 Murphy, J. G., Gregoire, P., Tevlin, A., Wentworth, G., Ellis, R., Markovic, M., & VandenBoer, T.
545 (2017). Observational constraints on particle acidity using measurements and modelling of
546 particles and gases [10.1039/C7FD00086C]. *Faraday Discussions*.
547 <https://doi.org/10.1039/C7FD00086C>
- 548 Nenes, A., Pandis, S. N., Kanakidou, M., Russell, A. G., Song, S., Vasilakos, P., & Weber, R. J. (2021).
549 Aerosol acidity and liquid water content regulate the dry deposition of inorganic reactive
550 nitrogen. *Atmos. Chem. Phys.*, 21(8), 6023-6033. <https://doi.org/10.5194/acp-21-6023-2021>
- 551 Nenes, A., Pandis, S. N., Weber, R. J., & Russell, A. (2020). Aerosol pH and liquid water content
552 determine when particulate matter is sensitive to ammonia and nitrate availability. *Atmos. Chem.*
553 *Phys.*, 20(5), 3249-3258. <https://doi.org/10.5194/acp-20-3249-2020>
- 554 Norman, M., Spirig, C., Wolff, V., Trebs, I., Flechard, C., Wisthaler, A., Schnitzhofer, R., Hansel, A., &
555 Neftel, A. (2009). Intercomparison of ammonia measurement techniques at an intensively
556 managed grassland site (Oensingen, Switzerland). *Atmospheric Chemistry and Physics*, 9(8),
557 2635-2645. <Go to ISI>://WOS:000265743100002
- 558 O'Dowd, C. D., & De Leeuw, G. (2007). Marine aerosol production: a review of the current knowledge.
559 *Philosophical Transactions of the Royal Society a-Mathematical Physical and Engineering*
560 *Sciences*, 365(1856), 1753-1774. <https://doi.org/10.1098/rsta.2007.2043>
- 561 Phillips, S. M., Bellcross, A. D., & Smith, G. D. (2017). Light Absorption by Brown Carbon in the
562 Southeastern United States is pH-dependent. *Environmental Science & Technology*.
563 <https://doi.org/10.1021/acs.est.7b01116>
- 564 Pinder, R. W., Adams, P. J., Pandis, S. N., & Gilliland, A. B. (2006). Temporally resolved ammonia
565 emission inventories: Current estimates, evaluation tools, and measurement needs. *Journal of*
566 *Geophysical Research-Atmospheres*, 111(D16), Article D16310.
567 <https://doi.org/10.1029/2005jd006603>
- 568 Pritchard, D. W. (1952). Salinity Distribution and Circulation in the Chesapeake Bay Estuarine System.
569 *Journal of Marine Research*, 11(2), 106-123. <Go to ISI>://WOS:A1952XR64900002
- 570 Pszenny, A. A. P., Moldanov, J., Keene, W. C., Sander, R., Maben, J. R., Martinez, M., Crutzen, P. J.,
571 Perner, D., & Prinn, R. G. (2004). Halogen cycling and aerosol pH in the Hawaiian marine
572 boundary layer. *Atmospheric Chemistry and Physics*, 4, 147-168. <https://doi.org/10.5194/acp-4-147-2004>
573

574 Pye, H. O. T., Nenes, A., Alexander, B., Ault, A. P., Barth, M. C., Clegg, S. L., Collett Jr, J. L., Fahey, K.
575 M., Hennigan, C. J., Herrmann, H., Kanakidou, M., Kelly, J. T., Ku, I. T., McNeill, V. F.,
576 Riemer, N., Schaefer, T., Shi, G., Tilgner, A., Walker, J. T., Wang, T., Weber, R., Xing, J.,
577 Zaveri, R. A., & Zuend, A. (2020). The acidity of atmospheric particles and clouds. *Atmos. Chem.*
578 *Phys.*, 20(8), 4809-4888. <https://doi.org/10.5194/acp-20-4809-2020>

579 Pye, H. O. T., Zuend, A., Fry, J. L., Isaacman-VanWertz, G., Capps, S. L., Appel, K. W., Foroutan, H.,
580 Xu, L., Ng, N. L., & Goldstein, A. H. (2018). Coupling of organic and inorganic aerosol systems
581 and the effect on gas-particle partitioning in the southeastern US. *Atmos. Chem. Phys.*, 18(1),
582 357-370. <https://doi.org/10.5194/acp-18-357-2018>

583 Rindelaub, J. D., Craig, R. L., Nandy, L., Bondy, A. L., Dutcher, C. S., Shepson, P. B., & Ault, A. P.
584 (2016). Direct Measurement of pH in Individual Particles via Raman Microspectroscopy and
585 Variation in Acidity with Relative Humidity. *J. Phys. Chem. A*, 120(6), 911-917.
586 <https://doi.org/10.1021/acs.jpca.5b12699>

587 Seinfeld, J. H., & Pandis, S. N. (2016). *Atmospheric chemistry and physics: from air pollution to climate*
588 *change* (3 ed.). John Wiley & Sons.

589 Tao, Y. (2020). *Identification of Major Factors Influencing Aerosol pH and the Quantitative Relationship*
590 *between pH and Ammonia Gas/Particle Partitioning* [University of Toronto]. University of
591 Toronto TSpace. <https://hdl.handle.net/1807/103788>

592 Tao, Y., & Murphy, J. G. (2019). The sensitivity of PM_{2.5} acidity to meteorological parameters and
593 chemical composition changes: 10-year records from six Canadian monitoring sites. *Atmos.*
594 *Chem. Phys.*, 19(14), 9309-9320. <https://doi.org/10.5194/acp-19-9309-2019>

595 Valerino, M. J., Johnson, J. J., Izumi, J., Orozco, D., Hoff, R. M., Delgado, R., & Hennigan, C. J. (2017).
596 Sources and composition of PM_{2.5} in the Colorado Front Range during the DISCOVER-AQ
597 study. *Journal of Geophysical Research-Atmospheres*, 122(1), 566-582.
598 <https://doi.org/10.1002/2016jd025830>

599 Vasilakos, P., Russell, A., Weber, R., & Nenes, A. (2018). Understanding nitrate formation in a world
600 with less sulfate. *Atmos. Chem. Phys.*, 18(17), 12765-12775. [https://doi.org/10.5194/acp-18-](https://doi.org/10.5194/acp-18-12765-2018)
601 [12765-2018](https://doi.org/10.5194/acp-18-12765-2018)

602 Weber, R. J., Guo, H., Russell, A. G., & Nenes, A. (2016). High aerosol acidity despite declining
603 atmospheric sulfate concentrations over the past 15 years [Letter]. *Nature Geoscience*, 9(4), 282-
604 285. <https://doi.org/10.1038/ngeo2665>

605 Zheng, G., Su, H., Wang, S., Andreae, M. O., Pöschl, U., & Cheng, Y. (2020). Multiphase buffer theory
606 explains contrasts in atmospheric aerosol acidity. *Science*, 369(6509), 1374.
607 <https://doi.org/10.1126/science.aba3719>

608